Global Change Biology (2001) **7**, 15–29

Assessing forest growth across southwestern Oregon under a range of current and future global change scenarios using a process model, 3-PG

N. C. COOPS* and R. H. WARING†
*CSIRO Forestry and Forest Products, Private Bag 10, Clayton South 3169, Melbourne Australia, †Oregon State University, College of Forestry, Corvallis, OR 97331, USA

Abstract

With improvements in mapping regional distributions of vegetation using satellite-derived information, there is an increasing interest in the assessment of current limitations on forest growth and in making projections of how productivity may be altered in response to changing climatic conditions and management policies. We utilised a simplified physiologically based process model (3-PG) across a 54 000 km^2 mountainous region of southwestern Oregon, USA, to evaluate the degree to which maximum periodic mean annual increment (PAI) of forests could be predicted at a set of 448 forest inventory plots. The survey data were pooled into six broad forest types (coastal rain forest, interior coast range forest, mixed conifer, dry-site Douglas-fir, subalpine forest, and pine forest) and compared to the 3-PG predictions at a spatial resolution of 1 km^2. We found good agreement ($r^2 = 0.84$) between mean PAI values of forest productivity for the six forest types with those obtained from field surveys. With confidence at this broader level of integration, we then ran model simulations to evaluate the constraints imposed by (i) soil fertility under current climatic conditions, (ii) the effect of doubling monthly precipitation across the region, and (iii) a widely used climatic change scenario that involves modifications in monthly mean temperatures and precipitation, as well as a doubling in atmospheric CO_2 concentrations. These analyses showed that optimum soil fertility would more than double growth, with the greatest response in the subalpine type and the least increase in the coastal rain forests. Doubling the precipitation increased productivity in the pine type (> 50%) with reduced responses elsewhere. The climate change scenario with doubled atmospheric CO_2 increased growth by 50% on average across all forest types, primarily as a result of a projected 33% increase in photosynthetic capacity. This modelling exercise indicates that, at a regional scale, a general relationship exists between simulated maximum leaf area index and maximum aboveground growth, supporting the contention that satellite-derived estimates of leaf area index may be good measures of the potential productivity of temperate evergreen forests.

Keywords: climate change, photosynthetic radiation, physiological modelling, regional analysis

Received 6 February 2000; revised version received and accepted 6 June 2000

Introduction

Regional-scale analyses are critical for many policy issues. With the availability of digital environmental datasets it is now possible to visualise some (but not all) of the implications of various policies before they are implemented. Although a variety of models are available that incorporate various types of data and make predictions about the consequences of changing climate and management on forests, few models have been tested against research-quality data before extrapolation.

We employed a general, physiologically based, forest growth model, **P**hysiological **P**rinciples **P**redicting **G**rowth (3-PG) (see Table 1 for a list of acronyms used in this paper) developed by Landsberg & Waring (1997).

Correspondence: N. C. Coops, fax +61/ 39545 8239, e-mail n.coops@ffp.csiro.au

Table 1 List of Acronyms

α_C	Quantum canopy efficiency
3-PG	Physiological Principles Predicting Growth
D	Vapour Pressure Deficit
DEM	Digital Elevation Model
FIA	Forest Inventory and Analysis
L	Leaf Area Index
PAI	Periodic Annual Increment
P_A	Aboveground biomass
P_B	Belowground biomass
P_F	Foliage biomass
P_G	Gross Primary Production
P_S	Stem biomass
P_N	Net primary production
VEMAP	Vegetation/Ecosystem Modelling and Analysis Project

This model was tested at 18 previously established research sites in southwestern Oregon (Coops *et al*. 1998; Coops *et al*. 2000), where detailed measurements of light, temperature, vapour pressure deficits, plant–water relationships, and bioassays of soil fertility had been acquired, along with measurements of site productivity (Waring & Cleary 1967; Cleary & Waring 1969; Waring 1969; Atzet & Waring 1970; Waring & Youngberg 1972; Reed & Waring 1974; Waring *et al*. 1975). There was good agreement between measured and simulated values of seasonal depletion in soil water and with site productivity ($r^2 > 0.75$). The model has also performed well in estimating wood production for a range of forest plantations on four continents (Landsberg *et al*. 2000) and the seasonal patterns in water vapour and carbon dioxide exchange recorded in a detailed study of a ponderosa pine forest (Law *et al*. 1999; Law *et al*. 2000). Therefore, we have general confidence in the model's performance and structure. We are also confident in our ability to extrapolate climatic conditions across diverse landscapes (Coops 2000; Coops *et al*. 2000b), so in this paper we have extended the analysis to an entire region where forest inventory data have been systematically acquired by the U.S. Forest Service and other federal agencies.

3-PG is process-based but has a number of simplifying assumptions, described below, that permit it to be driven with a minimum of information about forest structure, soil properties, and weather data. In this paper, we evaluate the growth potential of a range of forest types, under current conditions, and under a set of hypothetical future scenarios including:

- current temperatures with twice current monthly rainfall
- current climate with no nutrient limitations across the region
- future climate scenario with double current atmospheric CO_2

Methods

Study area

The Siskiyou Mountains, which extend from southern Oregon into northwestern California, represent a steep climatic gradient with annual precipitation decreasing from over 250 cm to less than 50 cm. Although the region is dominated by Douglas-fir [*Pseudotsuga menziesii* (Mirb.) Franco], the area is much drier than typical of the general Douglas-fir region in the Pacific North-West. The geology is also more complex, with the oldest parent materials dating back to the Silurian, more than 320 million years bp. There is a full range of igneous rocks, from acidic, silica-rich granites to the most ultrabasic peridotites. In addition, sedimentary and metamorphic rocks are widely represented. The most fertile soils are derived from graphite mica schist (Waring & Youngberg 1972), an unusual parent material, because it contains nitrogen in its matrix (Dahlgren 1994). The most infertile soils are derived from peridotite, and its metamorphic equivalent, serpentine (Irwin 1966).

In part because of the geological and climatic diversity, the Siskiyou Mountains contain many endemic species, with closer ties to flora in China and the Appalachian Mountains in the eastern USA than to other areas in western North America (Whittaker 1961). The area is particularly rich in conifers, with more than a dozen species present in some stands (Waring 1969). Jeffrey pine [*Pinus jeffreyi* (Grev. and Balf.)], which is near its northern limits, is restricted to soils derived from peridotite and serpentine.

3-PG model

The 3-PG model is based on a number of established biophysical relationships and constants. It is simple to apply because it involves few parameters, the values of which can be easily estimated from literature or from field measurements (see flow diagram of 3-PG in Table 2). 3-PG uses a monthly time-step; it requires as input data average daily short-wave incoming radiation for each month, mean daytime vapour pressure deficits, temperature extremes, total monthly precipitation and estimates of soil water storage capacity and fertility.

Absorbed photosynthetically active radiation ($\phi_{p.a}$) is estimated from global solar radiation derived, if necessary, from an established empirical relationship based on average maximum and minimum temperatures. The utilized portion of $\phi_{p.a}$ ($\phi_{p.a.u}$) is obtained by reducing $\phi_{p.a}$ by an amount determined by a series of modifiers

Table 2 Flow diagram of 3-PG

Inputs
- *Weather data*: temperature, precipitation, humidity, radiation, subfreezing days
- *Initial biomass*: foliage, stems, roots
- *Variables*: max.available soil water, initial stem number, stand age, max. stand age
- *Parameters*: canopy quantum efficiency, temperature optimum and limits for photosynthesis, ratio of P_A/P_G, max. leaf and canopy conductance, specific leaf area, maximum litterfall rate, root turnover rate (if soil carbon balance is of interest), soil fertility ranking, and parameters for the allometric equations

Model calculates monthly
- Leaf area index from foliage mass & specific leaf area and monthly litterfall
- Max. degree that a climatic variable limits stomatal or canopy conductance
- Transpiration from Penman–Monteith equation
- Gross photosynthesis from utilisable PAR multiplied by quantum efficiency
- Net primary production (P_N) as a fixed fraction of gross photosynthesis
- Fraction of P_N allocated to roots
- Fraction of P_A allocated to stems and foliage separately, using allometric equations with tree diameter

Model calculates annually
- Stem wood production (mass and volume)
- Net production, above and below ground
- Natural mortality and mortality through thinning
- Updates on tree biomass (alive and dead)
- Litter and root turnover
- Autotrophic respiration
- Relative constraint imposed by each environmental factor on production

(Landsberg & Gower 1997) derived from constraints imposed by (i) stomatal closure, associated with high day-time atmospheric vapour pressure deficits (D) (see Landsberg & Waring 1997); (ii) soil water balance, which is the difference between total monthly rainfall, plus available soil water stored from the previous month, and transpiration, calculated using the Penman-Monteith equation with canopy conductance (maximum value is set at $0.02\,m\,s^{-1}$) (Kelliher *et al*. 1995) modified by projected Leaf Area Index (L) of the forest and constrained by monthly estimates of D; (iii) the effects of subfreezing temperatures ($<-2\,°C$) using a frost modifier calculated from the number of frost days per month; and (iv) a temperature quadratic function that regulates the photosynthetic capacity seasonally.

The modifiers take values between 0 (system 'shut-down') and 1 (no constraint) (see Landsberg 1986; McMurtrie *et al*. 1994; Runyon *et al*. 1994). Gross primary production (P_G) is calculated by multiplying $\phi_{p.a.u.}$ by the canopy quantum efficiency (α_c). A major simplification in the 3-PG model is that it does not require calculation of respiration or root turnover, but assumes that total net primary production (P_N) in temperate forests is approximately a fixed fraction (0.47 ± 0.04) of P_G (Landsberg & Waring 1997; Arneth *et al*. 1998; Waring *et al*. 1998; Law *et al*. 1999). The model partitions an increasing fraction of P_N into belowground biomass (P_B) as environmental conditions become less favourable. The remaining P_N is partitioned into aboveground biomass (P_A), subdivided into two categories: stems (P_S) and foliage (P_F). Species-specific allometric equations related to changes in stem diameter are required to account for shifts P_S and P_F as trees grow. Calculation of the carbon partitioning coefficients is described in detail by Landsberg & Waring (1997), and also described by Landsberg *et al*. (2000). For convenience, the basic algebra is presented here. The ratio of the derivatives ($p_{f.s}$) describing foliage mass (w_f) and stem mass (w_s) in terms of stem diameter (B) is:

$$p_{f.s} = (dw_f/dB)/(dw_s/dB) =$$

$$a_f\, n_f\, B^{(n_f-1)}/a_s\, n_s\, B^{(n_s-1)} \quad (1)$$

This ratio determines the carbon allocation coefficients for foliage (η_f), roots (η_r) and stems (η_s) – which must sum to unity – through the relationships:

$$\eta_s = (1-\eta_f)/(p_{f.s}+1) \text{ and } \eta_f = 1-r-\eta_s. \quad (2)$$

The root allocation coefficient r varies with growing conditions, but for the purposes of evaluating the effects of varying values of a_s, n_s, a_f and n_f, r is taken as constant. The overall aim was to use as many standard default values for as many parameters as possible. The fraction of P_N allocated to root growth increases from 0.2 to 0.6 as the ratio $\phi_{p.a.u}/\phi_{p.a}$ decreases from 1.0 to 0.2.

A temperature function (T_f), which varies between zero and unity, was added to the model by Landsberg

et al. (2000) to take account of variations in monthly mean temperature (T_{mean}) that approach a threshold maximum (Th_{max}) or minimum (Th_{min}) departing from the temperature optimum (T_{opt}) for photosynthesis:

$$T_f = \frac{(T_{mean} - Th_{min})}{(T_{opt} - Th_{min})} \times \frac{(Th_{max} - T_{mean})}{(Th_{max} - T_{opt})} \left[\frac{(Th_{max} - T_{opt})}{(T_{opt} - Th_{min})} \right] \quad (3)$$

We chose coastal Douglas-fir as our reference species because it occurs, at least in small numbers, in all but the most extreme subalpine environments. Its temperature optimum is about 20 °C, with a minimum threshold of 0 °C and a maximum of 40 °C (Lewis *et al*. 1999).

Initial values of foliage, stem and root mass are also required, appropriate to the age of the stand at the beginning of a simulation, together with allometric equations for the species and soil parameters. The allometric equations for Douglas-fir are presented in Table 3. Landsberg *et al*. (2000) list additional allometric equations for other tree species that have been modelled with 3-PG. Leaf Area Index (L) is determined from foliage mass and estimates of specific leaf area (assumed here to be 6.0 m^2 kg^{-1}). In this study, we ran 3-PG with an initial stocking of 1000 seedlings ha^{-1}, with initial biomass of foliage, roots, and stems set at 1, 3, and 6 Mg ha^{-1}, respectively, the same values used by Landsberg & Waring (1997). The self-thinning routine was turned off, because fully stocked stands at maximum productivity (age 30–40 y) contain approximately 1000 trees ha^{-1} (McArdle 1961).

Sources of data

Climate. In order to assess the implications of changing climate and elevated atmospheric carbon dioxide concentrations, we relied on information available from the Vegetation/Ecosystem Modelling and Analysis Project (VEMAP 1995; Kittel *et al*. 1995, 1996; see http://www.cgd.ucar.edu/vemap). Two different sets of mean monthly temperature and precipitation data were acquired: a CURRENT climatic scenario based on a historical climate series, and a climate change scenario derived from coupled atmosphere–ocean global climate model experiments with transient greenhouse gas and sulphate aerosol forcing developed by the Hadley Centre for Climate Prediction and Research, UK (called the HADLEY climate). Both these datasets are a single years data (i.e. 12 months) and were developed for the contiguous United States and Alaska and released late in 1998 and early 1999. The datasets were provided at a resolution of 10 km^2 pixels and were terrain-adjusted using interpolation based on the PRISM system (Daly *et al*. 1994). We re-sampled the VEMAP climatic data to a spatial resolution of 1 km^2 using a bi-linear interpolation routine to match existing datasets and a digital elevation model (DEM) of the study area. The DEM for the study area is presented with survey plot locations (described below) in Fig. 1.

Temperature extremes and vapour pressure deficits. Existing PRISM estimates of current mean monthly temperature and precipitation of the region were available at 1 km^2 resolution. As only mean monthly temperature surfaces were available from the VEMAP project, a simple regression equation was developed from daily weather data acquired from stations within the study area to predict minimum and maximum values from the mean. We found that temperature extremes could be predicted with $r^2 = 0.97$ and an SE of prediction of 1.7 °C from daily and monthly mean temperatures.

From minimum temperatures each month, the frequency of frost was estimated using a linear relation developed by Coops *et al*. (2000a). Vapour pressure deficits were estimated by assuming that the dew point coincided with daily minimum temperatures, and that the daytime D is approximately 2/3 of the difference between saturated vapour pressure at the dewpoint and the saturated vapour pressure calculated for the maximum temperature (Coops *et al*. 2000b).

Radiation. Monthly estimates of total incoming shortwave radiation were calculated using models that first calculate the potential radiation reaching any spot, and then reduce the value based on the clarity (transmissivity) of the atmosphere (Goldberg *et al*. 1979; Bristow & Campbell 1984; Hungerford *et al*. 1989). Changes in the atmospheric transmissivity are mirrored in temperature extremes. With a DEM we adjusted for differences in slope, aspect, and elevation as well as for variations in the fraction of diffuse and direct solar beam radiation (Garnier & Ohmura 1968; Buffo *et al*. 1972; Swift 1976; Hungerford *et al*. 1989). Comparison with measured radiation data demonstrated that the modelling approach predicts both direct and diffuse components of mean monthly incoming radiation with 93–99% accuracy (Coops *et al*. 2000c). On slopes, the model accuracy was > 87% with a mean error of < 2 MJ m^{-2} d^{-1} (Coops *et al*. 2000c). Radiation estimates calculated for the current climate scenario were used thereafter for other scenarios because it was not possible with the data available to account for changes in cloud cover and minimum temperatures associated with varying precipitation. The monthly coverages were computed using the 1 km^2 resampled VEMAP climate surfaces and a 1-km^2 DEM allowing changes in aspect, slope and elevation to be account for.

Table 3 Model functions and parameters used for Douglas-fir in this study

Variable	Functions and Parameter Values Reference
Light conversion efficiency of photosynthesis	Maximum α_c ranges from 1.9 to 3.8 gC MJ^{-1} $\phi_{p.a.u}$, Landsberg (1986) increases linearly with soil fertility Waring (2000) Linder & Murray (1998)
Constraints of light conversion efficiency associated with temperature	T_{opt} was set at 20 °C, T_{min} 0 °C, and T_{max} 40 °C Lewis *et al*. (2000)
Fraction of radiation absorbed by canopy	$1-(2.718 \exp(-0.5^* L)$ Landsberg & Waring (1997)
Stomatal response to vapour pressure deficit	$g_c = g_{cmax} \exp(-2.5^* D)$ Landsberg & Waring (1997)
Specific Leaf Area	6.0 m^2 kg^{-1} Matson *et al*. (1994)
Allometric equation for stem mass	Stem mass, kg = 0.00075 exp (2.4 * dia., mm)
Allometric equation for foliage mass	Foliage mass, kg = 0.00045 exp (2.33 * dia., mm) This study
Wood density in stands < 20-year-old	400 kg m^{-3} Gholz 1982
Foliage turnover	0.017 month^{-1} 0.2 y $^{-1}$ Gholz 1982
Maximum leaf stomatal conductance	0.006 m s^{-1}
Maximum canopy stomatal conductance	0.02 m s^{-1}
Fraction of production allocated to roots, monthly	$0.8/(1+\phi_{p.a.u}/\phi_{p.a.})^*2.5^*$highest f_i Landsberg & Waring 1997 Selects the most restrictive environmental constraint (f_i), e.g. with value nearest zero; includes soil fertility

Symbols:
L = leaf area index, (m^2 m^{-2})
g_{cmax} = maximum stomatal conductance (m s^{-1})
$_{p.a}$ = photosynthetically active solar radiation (MJ m^{-2} month^{-1})
D = monthly mean daily vapour pressure deficit (kPa)
$_{p.a.u}$ = photosynthetically active solar radiation utilised (MJ m^{-2} month^{-1})
dia. = average stem diameter (mm)
T_{opt} = optimum temperature for photosynthesis
g_c = stomatal conductance (m s^{-1})

Soil fertility. For regional scale mapping and monitoring, the State Soil Geographic (STATSGO) database is the most appropriate because it has been compiled at a consistent scale for all USA states. Soil fertility was inferred principally from the STATSGO mineralogy classes that are provided in the description of major soil types, taking into account weathering losses of minerals associated with the age of the formation. We cross-referenced fertility ranking where possible using bioassays reported by Waring & Youngberg (1972). A total of 34 mineralogy classes are reported in the STATSGO database for the USA, of which 12 occur within the study area. These 12 classes were ranked from highest to lowest fertility using information from the additional STATSGO layers including soil type and broad scale land unit productivity. The canopy quantum efficiency (α_c) was modified as a function of soil fertility based on the work of Coops *et al*. 2000) and Waring 2000). Canopy quantum efficiency was increased linearly from 1.9 to 3.8 gC MJ^{-1} $\phi_{p.a.u}$ over the range of fertility derived from the STATSGO dataset.

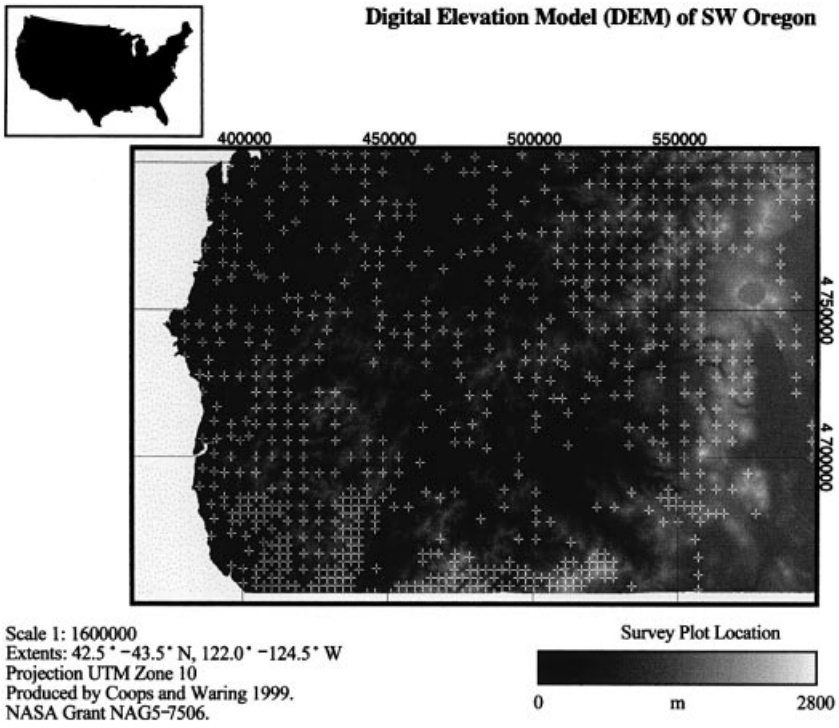

Fig. 1 Digital elevation map of study area with survey plot locations.

Soil water-holding capacity. For each STATSGO soil series, the depth of each soil horizon and its mean available soil water capacity (θ) were computed and summed for the entire profile to provide an estimate of θ for each 1 km^2 polygon. The mean values of θ from the STATSGO data were modified to account for the way drainage and soil depth vary with topography (Zheng *et al*. 1996; Coops & Waring 2000).

Forest survey data. The United States Forest Service (USFS) and the Bureau of Land Management (BLM) have a number of programs to determine the extent, condition, and volume of timber on private and public lands. Three sets of plots were used in this analysis: Forest Inventory and Analysis (FIA) plots located on private land, the Current Vegetation Surveys (CVS) also maintained by the USFS, and BLM plots. To assess the general accuracy of forest growth predictions by 3-PG under the CURRENT scenario, we relied on these three datasets (see Fig. 1 for plot locations in the region). For plots on federally owned land, data on standing volume, age, and height of dominant and co-dominant trees by species, at 10-year intervals, were acquired. We pooled the height and age information, regardless of species, and estimated the site index (m) (height at age 100 y) for coast-range Douglas-fir from standard yield tables (McArdle 1961). For plots located on private land, only limited data on individual tree were available so the average plot site index (based on McArdle for Douglas-fir) was used in the analysis. The yield tables gave values of maximum periodic mean annual increment (PAI) for fully stocked stands age 20–30 y, comparable to the specified output generated from the 3-PG model. By choosing maximum PAI at full stocking we were able to compare productivities across the range of surveyed stands, regardless of their present stocking, age, and vegetational composition. It is well established that Douglas-fir production is closely correlated with that of other tree species with which it occurs: Sitka spruce (*Picea sitchensis* (Bong.) Carr.) yields are 20% higher and those of ponderosa pine (*Pinus ponderosa* Doug. ex Loud.), 20% lower (Hann & Scrivani 1987).

Distribution of major forest types. We obtained data on the spatial distribution of current vegetation from the Oregon Gap Analysis Program. The analysis was based on LANDSAT^{TM} Multi-Spectral Scanner false-colour infrared positive prints acquired at a scale of 1:250 000. These prints were photo-interpreted, with supplemental information provided on the distribution of vegetation types from the U.S. Forest Service and Bureau of Land Management. Sixty-nine vegetation associations were defined for the State (Kagan & Caicco 1996). Only 16 of these associations were present in southwestern Oregon, and we combined these into six general forest types and assigned them, at a resolution of 1 km^2, over the study

Table 4 Dominant tree composition species in six, broadly defined forest types found in southwestern Oregon and site index statistics based on coast range Douglas-fir (McArdle 1961)

Forest type	Species	Mean site index (m) @ 100 years	Site index (m)		SE site index (m)	No. of survey plots
			Min.	Max.		
Coastal Rain	*Picea sitchensis – Tsuga heterophylla /Sequoia sempervirens*	35	27	46	1.3	24
Interior Coast Range	*Pseudotsuga menziesii – Lithocarpus densiflorus/ Acer macrophyllum – Alnus rubra-Pseudotsuga menziesii*	32	17	38	2.0	18
Dry Site Douglas-fir	*Pseudotsuga menziesii–Arbutus menziesii*	34	14	54	0.6	120
Mixed Conifer	*Pseudotsuga menziesii/Abies concolor–Abies grandis*	30	11	55	0.5	231
Subalpine	*Abies magnifica var. shastensis/ Tsuga mertensiana*	23	5	36	1.0	41
Pine	*Pinus ponderosa/Pinus jeffreyi*	24	17	30	1.1	14

Table 5 Modelled scenarios

Scenario/ forced simulation		3-PG modifications
Current climate	CURRENT	Minimum and maximum temperature (T) predicted from VEMAP mean monthly surfaces.
Current temperatures with twice current monthly rainfall	2*RAIN	Monthly rainfall surfaces * 2.0
Current climate with maximum fertility over entire region	MAXFERT	Fertility = maximum ($\alpha_c = 2.75$ gC MJ^{-1} $\phi_{p.a.u}$)
Future climate with double monthly T	HADLEY	Min/Max T predicted from HADLEY VEMAP mean
Solar radiation same as current CO_2	CURRENT	Canopy Quantum efficiency increased 33% from CURRENT

area. Table 4 lists the six broad forest types, their composition, statistics on survey plot sample size, and mean values and variation in site index.

Simulations

The 3-PG simulations were completed on a PC workstation using Arc/Info Geographic Information System (GIS) software with meteorological and soil data presented at a 1-km^2 spatial resolution. The CURRENT climatic scenarios involved providing 3-PG with a continual loop of the 12 months of current climate as published by VEMAP (1995). Model predictions were made from stand initiation plus 100 years. To compare predictions with ground-based measurements of site index, we extracted model predictions of maximum P_A, attained between age 20–30 y, and compared these with the maximum PAI extracted from McArdle (1961) yield tables. We also recorded maximum L predicted from the model for the same period.

In comparing yields predicted on the basis of the CURRENT climate and the future scenario predicted by HADLEY, we considered the effects of doubling current precipitation (2*RAIN) and maximizing soil fertility (MAXFERT) across the study area (Table 5). The latter two analyses represent potential management options, already in practice on some hybrid popular plantations within the region.

The HADLEY scenario includes doubling atmospheric CO_2. For evergreen conifers, we assumed that stomatal behaviour under this condition would not differ significantly from the present and that the major change would be an increase in canopy quantum efficiency (Ellsworth 1999). We increased the quantum efficiency by a third above that assumed in the CURRENT scenario, close to that suggested from experiments with Scots pine (*Pinus sylvestris* L.) (Overdieck *et al*. 1998), but more than double the response reported for Loblolly pine (*Pinus taeda* L.) under elevated CO_2 (Ellsworth 1999). The modelled response therefore should be considered near an

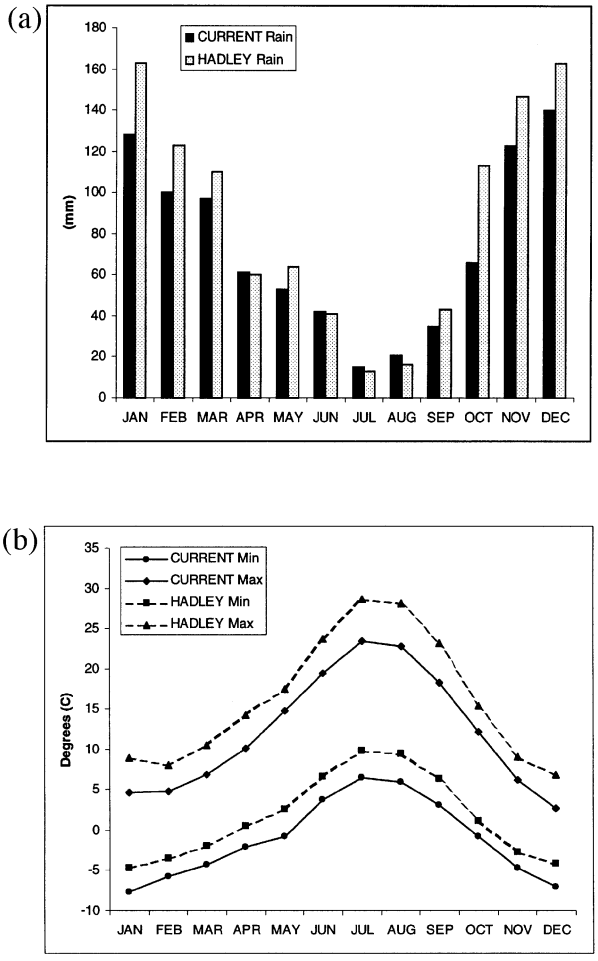

Fig. 2 Average monthly mean precipitation and temperature extremes for southwestern Oregon under CURRENT and future (HADLEY) scenarios.

upper limit, with more likely values perhaps as much as 50% lower (Lewis *et al*. 1999). The HADLEY scenarios involved providing 3-PG with a continual loop of 12 months of future climate (VEMAP 1995) from stand initiation plus 100 years (i.e no gradual change from CURRENT to HADLEY was modelled).

Results

CURRENT scenario

We compared 3-PG estimates of maximum periodic increment in stem volume growth under the CURRENT scenario by assuming a wood density of 400 kg m^{-3} (Gholz 1982). The survey plot data on site index, which totalled 448, were grouped into the six forest types and averaged (Table 3). Maximum PAI values were then extracted from Douglas-fir yield tables for stand ages between 30 and 40 y. These estimates of growth

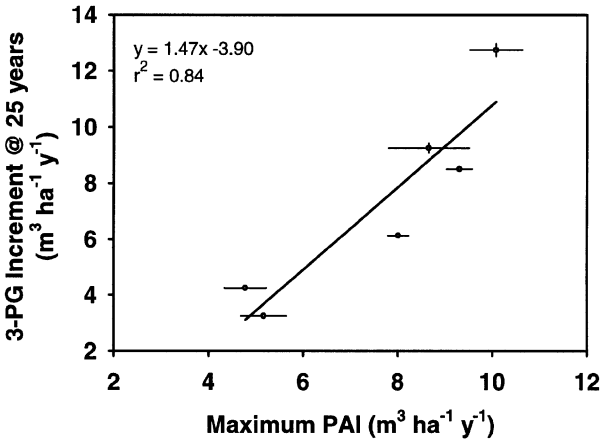

Fig. 3 Comparison of yield table-derived estimates of maximum periodic annual mean increment (PAI) obtained at the survey plots with aboveground biomass (P_A), stemwood volume generated by 3-PG under CURRENT climatic conditions.

compared well with 3-PG estimates made for the 1 km^2 cell nearest each survey plot when data were grouped into six major forest types ($r^2 = 0.84$, $P = < 0.01$, SE = 1.55 m^3 ha^{-1} y^{-1}; Fig. 3).

Table 6 lists the predicted maximum L and P_A for the six general forest types in southwestern Oregon using the CURRENT climate scenario and STATSGO spatial estimates of soil fertility and soil water holding capacity. These estimates represent averages acquired for all 1 km^2 cells that were mapped as containing the six representative forest types over the entire 54 000 km^2 region. If these average values are converted into volume increment (by multiplying by 2.5), we see that the large number of survey plots capture well the mean productivity estimates for each of the vegetation types (Fig. 3). For example the coastal rain forest estimates from the 24 sampled plots (14 vs. 13 m^3 ha^{-1} y^{-1}). For the mixed conifer type, with a sample size of 231 plots, the region-wide 3-PG average was within the error of estimate (8 vs. 6 m^3 ha^{-1} y^{-1}).

A sensitivity analysis was performed to assess limitations imposed by drought, vapour pressure deficits, and suboptimal and subfreezing temperatures under the current climate. Figure 4 presents the results of this analysis for the six forest types. Removing all temperature limitations has the greatest effect and by removing all soil water limitations on growth, 3-PG predicts a range of responses with a maximum increase in P_A of 400% at the pine forest type and a minimum of 150% for the coastal rain forest type. Constraints on growth associated with high vapour pressure deficits do not appear strong, but when this constraint is removed, transpiration increases, with the result that drought can become more restrictive and productivity remains essentially unchanged.

Table 6 Projected maximum Leaf Area Index (L) and maximum periodic annual increment of stemwood P_A (t dry mass $ha^{-1} y^{-1}$) under four scenarios with mean and standard errors (in parenthesis)

	CURRENT		2* RAIN		MAXFERT		HADLEY	
Forest types	L	P_A	L	P_A	L	P_A	L	P_A
Coastal Rain	7.0	5.6 (0.08)	11.0	5.8 (0.07)	10.5	7.8 (0.03)	12.6	6.5 (0.09)
Interior Coast Range	4.7	3.8 (0.06)	7.4	5.2 (0.07)	7.1	5.5 (0.06)	8.7	5.0 (0.06)
Dry Site Douglas-fir	4.1	3.3 (0.02)	6.3	4.6 (0.03)	6.7	5.1 (0.03)	7.5	5.2 (0.03)
Mixed Conifer	3.1	2.5 (0.01)	4.5	3.5 (0.02)	5.4	4.2 (0.02)	5.3	4.0 (0.02)
Subalpine	2.1	1.6 (0.02)	3.0	2.3 (0.03)	4.7	3.7 (0.02)	3.7	2.9 (0.02)
Pine	2.1	1.7 (0.02)	3.3	2.6 (0.04)	3.2	2.6 (0.03)	3.2	2.6 (0.03)

*CURRENT scenario with 2*RAIN*

If precipitation is doubled each month above current conditions, while other environmental variables are kept constant, 3-PG predicts that P_A will increase by less than 5% in the coastal rain forest to more than 50% in pine forests (Table 5, Fig. 5a).

CURRENT scenario with MAXIMUM FERTILITY (MAXFERT)

Soil fertility, as estimated from the STATSGO soil datasets, varies across the region, which results in α_c being assigned values from 1.9 to 3.8 $gC MJ^{-1}$ $\phi_{p.a.u}$. If all nutritional limitations were removed, 3-PG predicts increases in L and P_A of 40–50% in coastal rain forest and dry-site Douglas-fir types (Table 5, Fig. 5b). In contrast, subalpine forests might increase growth by >100%. The pine type is unlikely to respond as much because of limitations by drought and high vapour pressure deficits.

HADLEY scenario

To simulate a doubling of atmospheric CO_2 we increased the quantum canopy efficiency by 30% above the initial values assigned to all sites. This increase in canopy efficiency, together with increased rainfall and warmer temperatures resulted in higher values of L and P_A for all types (Table 5, Fig. 5a).

Discussion

Survey-based estimates of maximum PAI values compared well with 3-PG estimates when data were grouped into six major forest types. Maximum L estimates range from 7.0 for the coastal rain forests to around 2.0 for pine and subalpine forest types. Predicted P_A for these types follow similar trends with the coastal rain forests averaging maximum rates of 5.6 t of dry mass $ha^{-1} y^{-1}$, whereas pine and subalpine forests are predicted to produce between 1.6 and 1.7 t dry mass $ha^{-1} y^{-1}$ above ground, most of which is stemwood.

With general agreement between model predictions of maximum PAI under current climatic conditions and those predicted from yield tables, we have a basis for considering additional scenarios.

The sensitivity analysis allowed the limitations imposed by drought, vapour pressure deficits, and suboptimal and subfreezing temperatures under the current climate to be assessed. Analysis indicates the removal of all temperature limitations has the greatest effect, especially for the higher elevation types such as mixed conifer and subalpine forests. The effect on the coastal types, as a result of their already favourable climate, is less. The removal of all soil water limitations on growth results in a range of responses with a maximum increase in P_A of 400% at the pine forest type and a minimum of 150% for the coastal rain forest type. In contrast, growth constraints associated with high vapour pressure deficits do not appear strong, because when this constraint is removed, transpiration increases, with the result that drought can become more restrictive and productivity remains essentially unchanged.

If precipitation is doubled each month above current conditions, while other environmental variables are kept constant L increased from 7 to 11 in the rain forest type and from 1.7 to 3.3 in the drier pine type. The increase in P_A tends to increase proportionally to increased L, with

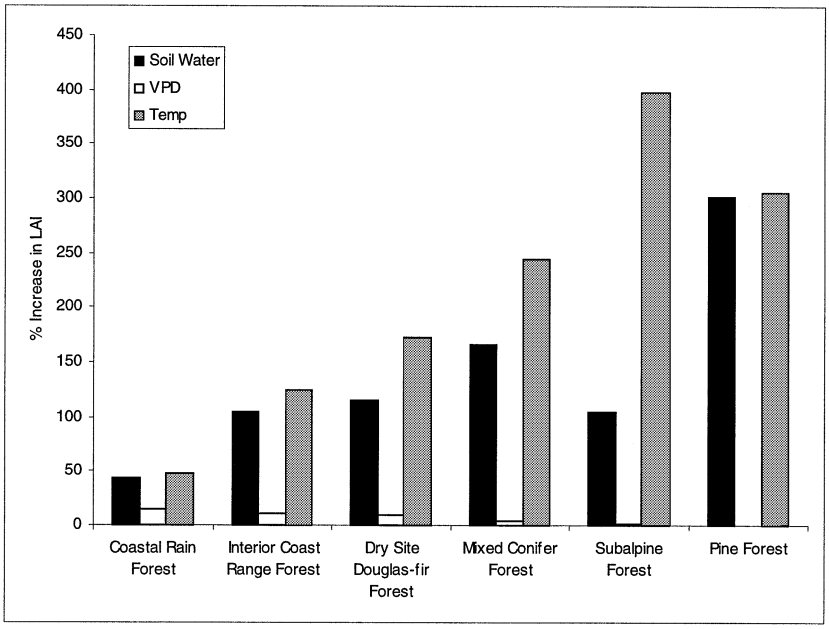

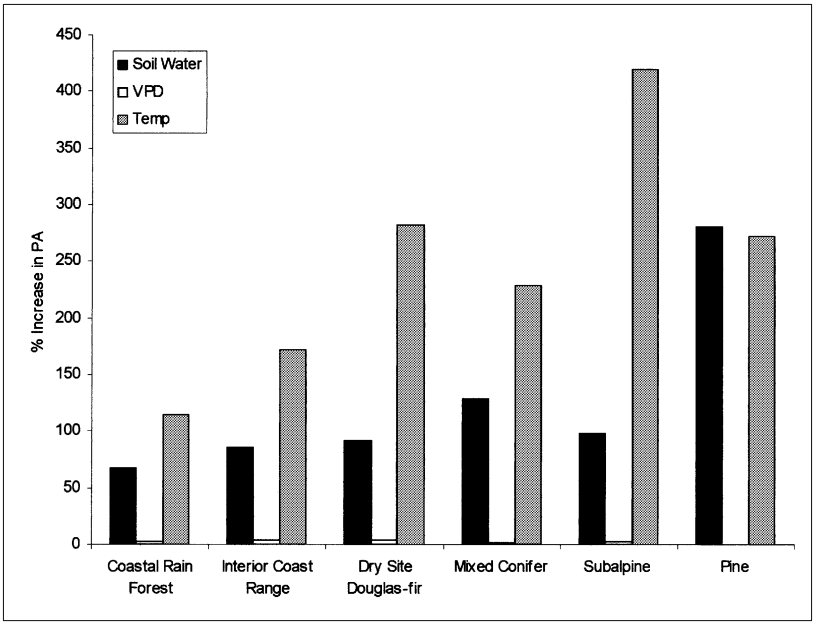

Fig. 4 Modelled changes of leaf area index (L) and with aboveground biomass (P_A) for the six forest types under CURRENT climate with soil water, vapour pressure deficit and temperature restrictions separately removed.

the exception of the coastal rain forest, where the effects of drought are currently minor, and an increase in L would intercept little more additional radiation. If all nutritional limitations were removed L and P_A increases 40–50% in coastal rain forest and dry-site Douglas-fir types, however, the subalpine forests might increase growth by > 100%.

The HADLEY scenario result is similar to that predicted by doubling the precipitation under current climatic conditions with L increasing, in most cases by greater than 60% and P_A increasing from 15% for the coastal rain forest to nearly 80% for the subalpine type. If, however, we assume that the 5–10% increase in quantum efficiency reported for Douglas-fir seedlings exposed to enhanced CO_2 is more likely (Lewis *et al*. 1999), the overall response would be closer to 20%, matching similar studies (Pan *et al*. 1998).

The importance of temperature on restricting forest growth over the region diminished under the HADLEY scenario, primarily in response to higher minimum temperature. This increase in temperature, however, increases constraints from D on all six types as compared

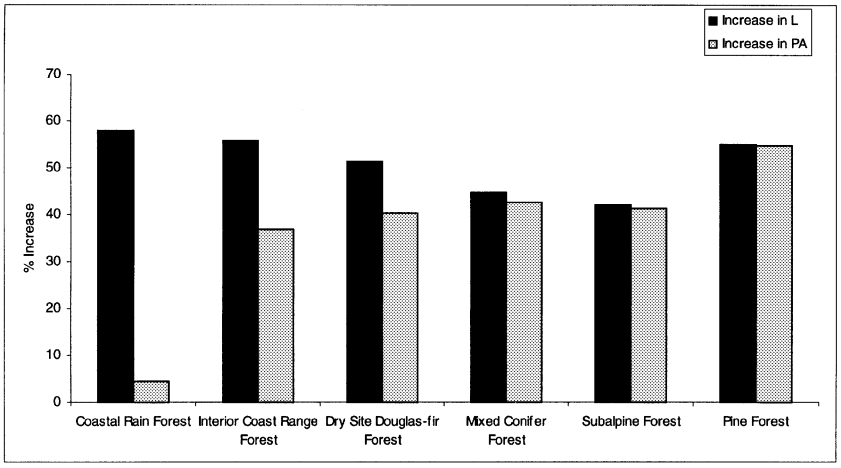

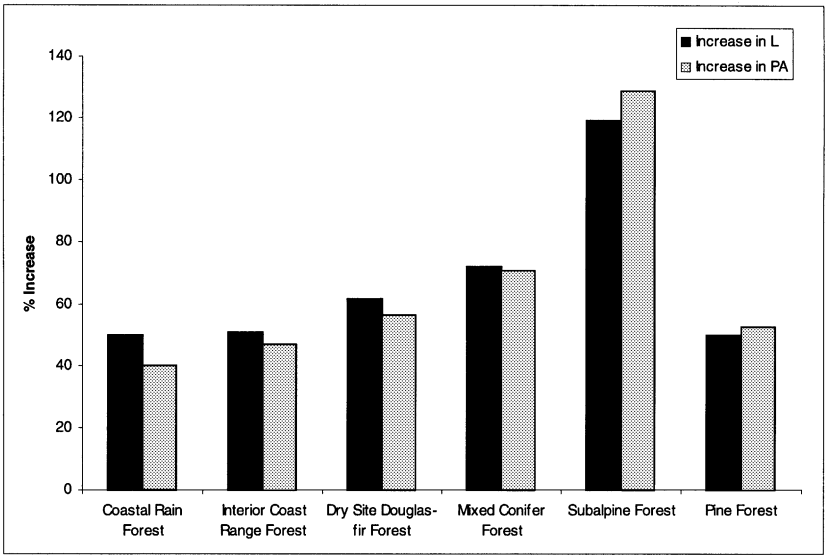

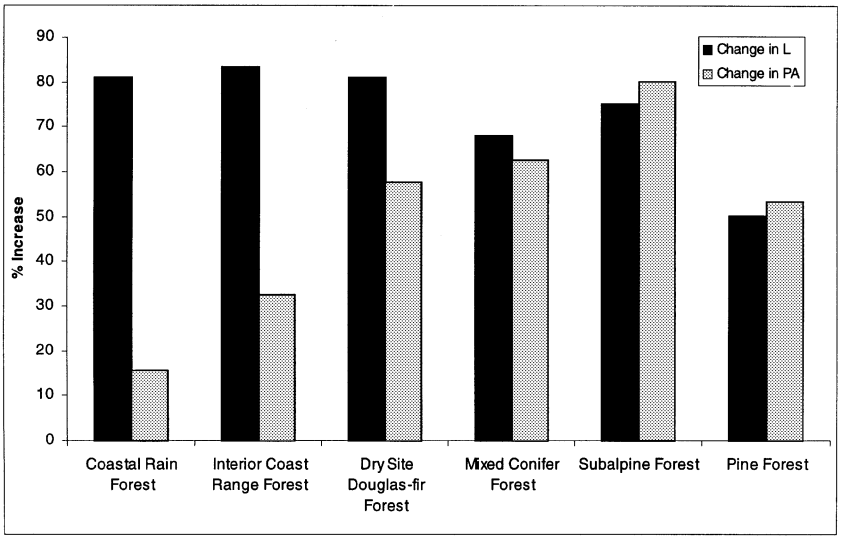

Fig. 5 Percentage change in leaf area index (L) and with aboveground biomass (P_A) for the six vegetation types using (a) the 2*RAIN climatic scenario, and (b) the MAXFERT scenario and (c) the HADLEY scenario.

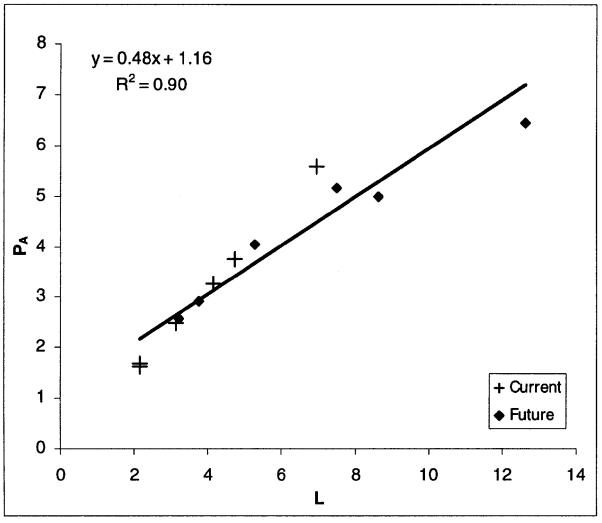

Fig. 6 The relationship between leaf area index (L) and with aboveground biomass (P_A) for the six different vegetation types, averaged over the entire region for the CURRENT and the HADLEY scenarios.

to the CURRENT scenario. In some cases, predicted changes in precipitation increased water stress, as in the pine and interior coast range types. In other cases, such as for the subalpine and the coastal rain forests, changes in precipitation had little predicted effect (data not shown).

Gholz (1982) was the first to demonstrate a general relationship between maximum L and aboveground primary production across a broad range of coniferous forests in Oregon. We cannot assume that this relationship will remain constant as forests age, but maximum leaf area is a variable that can be predicted from space using broad or refined spectral indices (Goward *et al*. 1994; Running *et al*. 1994; Waring & Running 1998; Coops 1999) and it has considerable value for predicting the productive capacity of the landscape. From our results, modelling both current and future climatic scenarios, we found a general relationship between maximum L and maximum PAI for the broad forest types with an $r^2 = 0.9$ (Fig. 6). This suggests that predicted changes in growth, as well as maximum L, may be in the future be confirmed or rejected on the basis of satellite-derived information.

Although 'greener' forests are predicted for most of the scenarios when compared to current conditions, stemwood production is not always commensurate with simulated increase in L. This type of response is a consequence, in part, of the small increase in light interception once $L > 5$, at which 92% of $\phi_{p.a}$ is intercepted. On drought-prone sites, which generally have $L < 2$, an increase in canopy results in greater interception of precipitation and an increase in transpiration. As a result, an increased fraction of P_N is partitioned to roots and less is available for stem growth. In general, however, scenarios that increase α_c, such as MAXFERT and HADLEY, result in an increase in both foliage and stem production. We believe that the likelihood of α_c responding to doubling CO_2 is, however, unrealistically high. Recent studies indicate for Douglas-fir no shift in photosynthetic capacity (or respiration) with a 50% increase in ambient CO_2 (Lewis *et al*. 1999)

Limitations in the coverage of the survey dataset are apparent from inspection of Fig. 1. Less obvious, but equally constraining for precise analysis, is a policy of the U.S. Federal Government to offset the true location of stands on private land. In addition, the climatic scenarios were provided at a large scale, 10 km^2, which in many cases proved too broad to define the climatic conditions accurately in highly mountainous topography and for the narrow band of coastal rain forests.

The quality of the climatic data is a source of concern. When a climate change scenario predicts more or less precipitation, we need to know whether cloud cover will change. We assumed in this paper that only the intensity of storms increased. If, however, the frequency increased, there would be more cloud cover and consequent significant reductions in solar radiation and vapour pressure deficit from those assumed. As demonstrated by modelling at monthly time-steps, the distribution of precipitation in a drought-prone region is often more important than the total amount.

Soils data are essentially non-quantitative and at scales of 1 km^2 or larger, generally fail to recognise significant changes in parent material. Even with more precise mapping, the actual fertility of forest soils would be difficult to judge. Many areas have been commercially fertilized, others have supported vegetation with the capacity to fix nitrogen, and in some locations atmospheric deposition of nutrients (and pollutants) affect the soil fertility in ways unrecorded by general soil surveys.

Nevertheless, the modelling analysis indicates that at a regional scale, local estimates of growth by forest type, when averaged, are closely correlated with averaged survey plot values of maximum PAI derived from yield tables (Fig. 3), recognizing that the absolute values are lower in the Siskiyous Mountains than for yield tables developed for Douglas-fir in the Coast Range (Dr David Hann, Department of Forest Resources, Oregon State University). It might be desirable to have separate yield tables for all the major species, although to model with this refinement would require additional physiology and structural information similar to that listed for Douglas-fir in Table 2.

There has recently been an increased effort to compare a wide variety of simulation models at regional and global scales (see *Global Change Biology*, 5, The Postdam

NPP Model Intercomparison; Pan *et al*. 1998). Although valuable in identifying differences between models, the ground-based data available are generally inadequate to explain why model predictions differ. In order to gain further and better insights into model performance and differences we recommend that model comparisons be concentrated on sites where high-quality meteorological data are combined with seasonal measurements of energy and carbon exchange (Law *et al*. 2000).

Ultimately, remote sensing will play an increasing role in helping to parameterize models and confirm some predictions. It is anticipated that recent and new satellite programs, such as the Tropical Rainfall Measuring Mission (TRMM), and CERES (Clouds and the Earth's Radiant Energy System), combined with the upcoming launch of CLOUDSAT (a multisatellite, multisensor experiment due for launch by NASA in 2003), will provide unprecedented capabilities for deriving precipitation and surface long-wave radiation from space. Understanding the error characteristics of such retrievals, particularly at longer timescales over large areas, will be crucial to achieving a definitive evaluation of the sensitivity of the global climate models. Fully utilising such observations will require a comprehensive research effort, one that acknowledges the coupled nature of the hydrologic, carbon, and nutrient budgets. Although remote sensing cannot evaluate soil properties directly, it may be possible to assess the extent and magnitude of drought and seasonal variation in photosynthetic capacity of vegetation (Waring & Running 1999). It may also be possible, using LIDAR (LIght Detection And Ranging technology), to monitor changes in net aboveground production at local and regional scales (Lefsky *et al*. 1997; Lefsky *et al*. 1999; Means *et al*. 1999).

Acknowledgements

We wish to acknowledge Dr Joe Landsberg for discussions concerning the application of 3-PG. We also thank Dr Ron Neilson and Dr Ray Drapek (USFS) for useful discussions and for providing the basic information for extrapolation of minimum/maximum temperature and precipitation for CURRENT and HADLEY climate change scenarios. Dr Janet Ohmann provided the forestry survey datasets and useful advice. Mr Stephen Brown prepared the DEM for analysis. Drs' Landsberg, Neilson and Ohmann also provided valuable comments on drafts of this manuscript. We are also grateful for the comments from 2 anonymous reviewers.

Part of this research (NCC) was undertaken at Department of Forest Science, Oregon State University, Oregon whilst Dr Coops was on leave from CSIRO Forestry and Forest Products, Australia. The research reported in this article was supported by funds from the National Aeronautics and Space Administration (NASA) Grant Number NAG5-7506.

Additional information on this research is available at http://www.fsl.orst.edu/bevr or http://www.ffp.csiro.au/nfm/mdp.

References

Arneth A, Kelliher FM, McSeveny TM, Byers J (1998) Net ecosystem productivity, net primary productivity and ecosystem carbon sequestration in *Pinus radiata* plantation subject to soil water deficit. *Tree Physiology*, **18,** 785–793.

Atzet T, Waring RH (1970) Selective filtering of light by coniferous forests and minimum light energy requirements for regeneration. *Canadian Journal of Botany*, **48,** 2163–2167.

Bristow KL, Campbell GS (1984) On the relationship between incoming solar radiation and daily maximum and minimum temperature. *Agricultural and Forest Meteorology*, **31,** 159–166.

Buffo J, Fritschen L, Murphy J (1972) *Direct solar radiation on various slopes from 0° to 60° north latitude. Research Paper PAW-142.* US Department of Agriculture Forest Service, Portland, OR, 74pp.

Cleary BD, Waring RH (1969) Temperature: collection of data and its analysis for the interpretation of plant growth and distribution. *Canadian Journal of Botany*, **47,** 167–173.

Coops NC (1999) Linking multi-resolution satellite-derived estimates of canopy photosynthetic capacity and meteorological data to assess forest productivity in a *Pinus radiata* (D. Don) stand. *Photogrammetric Engineering and Remote Sensing*, **65,** 1149–1156.

Coops NC (2000) Comparison of topographic and physiographic properties measured on the ground with those derived from digital elevation models. *Northwest Science*, **74,** 116–130.

Coops NC, Waring RH (2000) Estimating maximum potential site productivity and site water stress of the Eastern Siskiyous using 3-PGS. *Canadian Journal of Forest Research*, in press.

Coops NC, Phillips N, Waring RH, Landsberg JJ (2000a) Prediction of solar radiation, vapor pressure deficit, and occurrence of frost from mean daily temperature extremes. *Agriculture and Forest Meteorology*, in review.

Coops NC, Waring RH, Landsberg JJ (1998) Assessing forest productivity in Australia and New Zealand using a physiologically-based model driven with averaged monthly weather data and satellite derived estimates of canopy photosynthetic capacity. *Forest Ecology and Management*, **104,** 113–127.

Coops NC, Waring RH, Landsberg JJ (2000b) Estimation of potential forest productivity across the Oregon transect using satellite data and monthly weather records. *International Journal of Remote Sensing*, in press.

Coops NC, Waring RH, Moncrieff J (2000c) Estimating Mean Monthly Incident Solar Radiation on Horizontal and Inclined Slopes from Mean Monthly Temperatures Extremes. *Journal of Biometeorology*, **44,** 201–211.

Dahlgren RA (1994) Soil acidification and nitrogen saturation from weathering of ammonium-bearing rock. *Nature*, **368,** 838–841.

Daly C, Neilson RP, Phillips DL (1994) A statistical-topographic model for mapping climatological precipitation over mountainous terrain. *Journal of Applied Meteorology*, **33,** 140–158.

Ellsworth DS (1999) CO_2 enrichment in a maturing pine forest: are CO_2 exchange and water status in the canopy affected? *Plant, Cell and Environment*, **22,** 461–472.

Garnier BJ, Ohmura A (1968) A method for calculating the direct shortwave radiation income on slopes. *Journal of Applied Meteorology*, **7,** 796–800.

Gholz HL (1982) Environmental limits on aboveground net primary productivity, leaf area and biomass in vegetation zones of the Pacific Northwest. *Ecology*, **63,** 469–481.

Goldberg B, Klein WH, McCartney RD (1979) A comparison of some simple models used to predict solar irradiance on a horizontal surface. *Solar Energy*, **23,** 81–83.

Goward SN, Waring RH, Dye DG, Yang J (1994) Ecological remote sensing at OTTER: Satellite macroscale observations. *Ecological Applications*, **4,** 322–343.

Hann DW, Scrivani JA (1987) *Dominant-height-growth and site-index equations for Douglas-fir and ponderosa pine in southwest Oregon.* Research Bulletin 59. Oregon State University, Forest Research Laboratory, Corvallis, OR.

Hungerford RD, Nemani RR, Running SW, Coughlan JC (1989) *MTCLIM: A mountain microclimate simulation model.* Research Paper INT0414. United States Department of Agriculture, Ogden, UT, 52pp.

Irwin WP (1966) Geology of Klamath Mountains province. In: *Geology of Northern California* (ed. Bailey EH). *Californian Division of Mines & Geology Bulletin*, **190**, 19–38.

Kagan J, Caicco S (1996) *Manual of Oregon actual vegetation. Oregon Gap Analysis Program.* U.S. Fish and Wildlife Service, Portland, OR.

Kelliher FM, Leaning R, Raupach MR, Schulze ED (1995) Maximum conductance for evaporation from global vegetation types. *Agricultural and Forest Meteorology*, **73,** 1–16.

Kittel TGF, Rosenbloom NA, Painter TH *et al.* (1996) The VEMAP Phase I database: An integrated input dataset for ecosystem and vegetation modeling for the conterminous United States (CD-ROM and online). http://www.cgd.ucar.-edu/vemap.

Kittel TGF, Rosenbloom NA, Painter TH, Schimel DS, VEMAP Modeling Participants (1995) The VEMAP integrated database for modeling United States ecosystem/vegetation sensitivity to climate change. *Journal of Biogeography*, **22,** 857–862.

Landsberg JJ (1986) *Physiological Ecology of Forest Production*. Academic Press, Sydney.

Landsberg JJ, Gower ST (1997) *Applications of Physiological Ecology to Forest Management*. Academic Press, San Diego, CA, 354pp.

Landsberg JJ, Waring RH (1997) A generalized model of forest productivity using simplified concepts of radiation-use efficiency, carbon balance, and partitioning. *Forest Ecology and Management*, **95,** 209–228.

Landsberg JJ, Waring RH, Coops NC (2000) Performance of the forest productivity model 3-PG applied to a wide range of forest types. I. Model structure, calibration and sensitivity analysis. *Forest Ecology and Management*, in review.

Law BE, Baldocchi DD, Anthoni PM (1999) Below-canopy and soil CO_2 fluxes in a ponderosa pine forest. *Agricultural Forest Meteorology*, **94,** 171–188.

Law BE, Waring RH, Aber JD, Anthoni PM (2000) Measurements of gross and net ecosystem productivity and water vapour exchange of a *Pinus ponderosa* ecosystem, and an evaluation of two generalized models. *Global Change Biology*, **6,** 155–168.

Lefsky MA, Cohen WB, Acker SA, Spies TA, Parker GG, Harding D (1997) LIDAR remote sensing of forest canopy structure and related biophysical parameters at the H.J. Andrews Experimental Forest, Oregon, USA. In: *Natural Resources Management using Remote Sensing and GIS* (ed. Greer JD). ASPRS, Washington, DC.

Lefsky MA, Harding D, Cohen WB, Parker G, Shugart HH (1999) Surface LIDAR remote sensing of basal area and biomass in deciduous forests of eastern Maryland, USA. *Remote Sensing of Environment*, **67,** 83–98.

Lewis JD, Olszyk D, Tingey DT (1999) Seasonal patterns of photosynthesis in Douglas-fir seedlings during the third and fourth year of exposure to elevated carbon dioxide and temperature. *Tree Physiology*, **19,** 243–252.

Matson P, Johnson L, Billow C, Miller J, Pu R (1994) Seasonal patterns and remote spectral estimation of canopy chemistry across the Oregon transect. *Ecological Applications*, **4,** 280–298.

McArdle RE (1961) *The Yield of Douglas-fir in the Pacific Northwest.* Technical Bulletin 201. USDA, Washington, DC.

McMurtrie RE, Gholz HL, Linder S, Gower ST (1994) Climatic factors controlling the productivity of pine stands: a model-based analysis. *Ecological Bulletins*, **43,** 173–188.

Means JE, Acker SA, Harding DJ *et al.* (1999) Use of large-footprint scanning airborne Lidar to estimate forest stand characteristics in the western Cascades of Oregon. *Remote Sensing of Environment*, **67,** 298–308.

Overdieck D, Kellomaki S, Wang KY (1998) Do the effects of temperature and CO_2. In: *European Forests and Global Change* (ed. Jarvis PG). Cambridge University Press, London.

Pan Y, Melillo JM, McGuire AD *et al.* (1998) Modeled responses of terrestrial ecosystems to elevated atmospheric CO_2: a comparison of simulations by the biogeochemistry models of the vegetation/ecosystem modeling and analysis project (VEMAP). *Oecologia*, **114,** 389–404.

Reed KL, Waring RH (1974) Coupling of environment to plant response: a simulation model of transpiration. *Ecology*, **55,** 62–72.

Running SW, Justice CO, Salomonson V *et al.* (1994) Terrestrial remote sensing science and algorithms planned for EOS/MODIS. *International Journal of Remote Sensing*, **15,** 3587–3620.

Runyon J, Waring RH, Goward SN, Welles JM (1994) Environmental limits on net primary production and light-use efficiency across the Oregon transect. *Ecological Applications*, **4,** 226–237.

Swift LW (1976) Algorithm for solar radiation on mountain slopes. *Water Resources Research*, **121,** 108–112.

VEMAP Members (Melillo JM, Borchers J Chaney J *et al.*) (1995) Vegetation/Ecosystem Modeling and Analysis Project (VEMAP): Comparing biogeography and biogeochemistry models in a continental-scale study of terrestrial ecosystem responses to climate change and CO_2 doubling. *Global Biogeochemical Cycles*, **9,** 407–437.

Waring RH (1969) Forest plants of the eastern Siskiyous: their environmental and vegetational distribution. *Northwest Science*, **43,** 1–17.

Waring RH (2000) A process model analysis of environmental limitations on the growth of Sitka spruce plantations in Great Britain. *Forestry*, **75,** 65–79.

Waring RH, Cleary BD (1967) Plant moisture stress: evaluation by pressure bomb. *Science*, **155,** 1248–1254.

Waring RH, Running SW (1998). *Forest Ecosystems: Analysis at Multiple Scales*. Academic Press, San Diego, CA.

Waring RH, Running SW (1999) Remote sensing requirements to drive ecosystem models at the landscape and regional scale. In: *Integrating Hydrology, Ecosystem Dynamics, and Biogeochemistry in Complex Landscapes* (eds Tenhunen JD, Kabat P), pp. 23–38. Wiley, New York.

Waring RH, Youngberg CT (1972) Evaluating forest sites for

potential growth response of trees to fertilizer. *Northwest Science*, **46,** 67–75.

Waring RH, Emmingham WH, Running SW (1975) Environmental limits of an endemic spruce, *Picea breweriana*. *Canadian Journal of Botany*, **53,** 1599–1613.

Waring RH, Landsberg JJ, Williams M (1998) Net primary production of forests: a constant fraction of gross primary production? *Tree Physiology*, **18,** 129–134.

Whittaker RH (1961) Vegetation history of the Pacific Coast States and the 'central' significance of the Klamath region. *Madrono*, **16,** 5–23.

Zheng D, Hunt ER, Running SW (1996) Comparison of available soil water capacity estimated from topography and soil series information. *Landscape Ecology*, **11,** 3–14.